REAL TIME OBJECT TRACKING ON GPGPU*

Maciej Chociej and Adam Polak
Theoretical Computer Science Department, Faculty of Mathematics and Computer Science, Jagiellonian University, Kraków, Poland

Keywords: Motion Tracking, GPGPU, Optical Flow, Foreground Separation.

Abstract: We propose a system for tracking objects in a video stream from a stationary camera. Our method, as often used, involves foreground-background separation and optical flow calculation. The major finding is fast feedback process that leads to an accurate detection of background-object and object-object boundaries and maintaining them during object occlusions. The contribution of this paper also includes improvements to computing dense optical flow and foreground separation. The methods described were implemented on a GPGPU and yield performance results sufficient for real time processing. Additionally, our approach makes no a priori assumptions on the characteristics of tracked objects and can be utilized to track both rigid and deformable objects of various shapes and sizes.

1 INTRODUCTION

Object tracking is one of central problems in computer vision. Robust tracking algorithms need to combine techniques from many areas of the field. Questions that need to be answered are:

- what are the objects we want to track;
- what are the cues that allow us to separate an object of our interest from its surroundings;
- what abstractions to model an object with and how to maintain their correspondence in time.

Even more questions arise when motion is taken into account:

- how to detect movement accurately and fast in terms of computation time;
- how should detection of movement influence the way we partition objects in the image space;
- can we through motion analysis distinguish between objects that are involved in complicated, dynamic interactions.

The literature on the subject is vast and presents many methods that respond to most of these questions. In a recent survey (Yilmazr et al., 2006) tracking algorithms are divided based on the representation of the objects as: a single point or points, simplified geometric shapes, object contours and silhouettes and articulated shape models constructed from the former types. In (Bugeaue and Pérezz, 2008) the authors reassign those algorithms to three distinct groups: detect-before-track, track and combine partitions and the third group: track distinct features or feature distributions. The first type of algorithms relies on external schemes that detect classes of well known objects (license plates (Donoser et al., 2007)(Zweng and Kampel, 2009), vehicles (Feris et al., 2011), humans and human faces (Karlsson et al., 2008)(Wu and Nevatia, 2007) and describe them in terms of simple structures like points or bounding boxes, which then can be tracked over time. The second type is based on a primary detection of objects, possibly by external means. Such objects silhouettes, usually represented by the contour or an energy function in the image space, are then evolved to meet specific energy preservation criteria. The last group consists of algorithms focusing on the detection and tracking of unique features in the appearance of the objects and by their movement predicting and extrapolating the movement of an object as a whole.

The paper (Bugeaue and Pérezz, 2008) contains an interesting review of those three types of algorithms, their strengths and drawbacks and proposes a hybrid method combining those approaches. Our method is based on similar premises, but varies significantly in details. By exploiting the power of GPG-

*This paper is based on work funded by Polish Ministry of Science and Higher Education (grant R00 0081 11) in cooperation with AutoID Polska S.A.

Chociej M. and Polak A..
REAL TIME OBJECT TRACKING ON GPGPU.
DOI: 10.5220/0003862303030310
In *Proceedings of the International Conference on Computer Vision Theory and Applications* (VISAPP-2012), pages 303-310
ISBN: 978-989-8565-04-4

PUs we compute dense optical flow that allows us to predict object deformations with higher precision. The quality of our optical flow also makes us less dependent on detecting 'observations' (in the sense of (Bugeaue and Pérezz, 2008)), as object identification can be propagated for much longer time. Finally in (Bugeaue and Pérezz, 2008) object distinction is performed via multiple graph-cuts, whereas we employ a delayed voting scheme. In the scenario with a stationary camera this allows us to process high resolution inputs with real-time performance and comparable accuracy.

It is worth to mention that there exist another approach to combine the three mentioned types of algorithms, i.e. data fusion (Makris et al., 2011).

2 THE PROBLEM

In this paper we propose a method that can be used to solve the following basic problem: In each frame of a given video stream we want to separate moving objects and assign to them unique identifiers. These identifiers should be discovered as soon as the object appears in the view and should be held as long as the object is visible.

An additional goal is to strike a proper balance between the precision and the computational cost. We strove for real-time performance and thus decided to focus on algorithms where natural data parallelism in the image space could be exploited.

Our method is intended to work at the lowest level of a more complex tracking system. It is designed to be easily integrated with higher level logic capable of handling more difficult object-object interactions.

We define an object as a group of pixels forming a connected component of the input image and moving in a coherent way. We do not make any other assumptions about tracked objects. This makes our method general and versatile, capable of tracking humans in motion, vehicles, as well as other moving objects, both rigid and deformable. However, we require that the camera is stationary and that it is, without losing generality, in an upright orientation.

When tracking the objects we face the following major problems which need to be solved:

- detecting new objects, and separating them from the background;
- resolving object occlusion;
- separating objects which move together in close proximity in the same direction;
- splitting objects which we incorrectly tracked as a single one;
- joining objects which we detected separately but seem to be parts of one physical entity.

We have implemented our method on multicore CPUs and CUDA based GPGPUs and performed extensive tests that included footage from various indoor and outdoor scenarios. These tests had shown that our approach handles with reasonable accuracy all these cases, apart from the last one – joining object parts. We leave this to be solved with higher level logic, which is the goal of our future work.

3 METHOD OVERVIEW

The main modules our method consists of are presented in the figure below. It is followed by the general description of these modules.

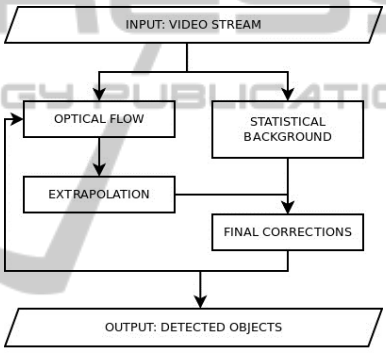

Figure 1: Block diagram of our method.

Our procedure processes consecutive frames appearing in the video stream. After the frame is processed we return its partition into a number of tracked objects and the background.

When the new frame appears in the video stream, we process it as follows:

1. **Optical Flow.** We compute the optical flow between the previous and the current frame. The method we use exploits the object partition computed for the previous frame.
2. **Extrapolation.** We predict the location of tracked objects in the current frame using the computed optical flow and the previous frame.
3. **Statistical Background.** We compute the foreground-background separation in the current frame based on statistical model of the background.
4. **Final Corrections.** We apply small corrections to the extrapolated partition from the second step. These include:

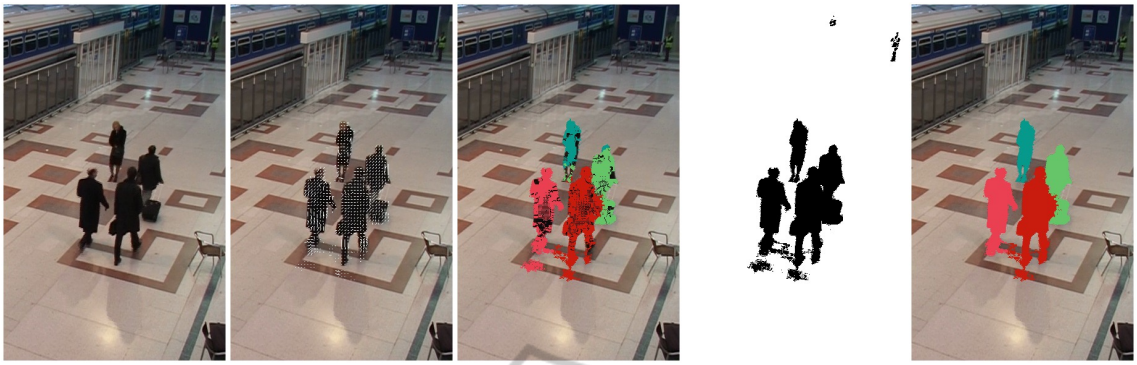

Figure 2: An example frame from the PETS 2006 dataset, left to right: the original frame, the optical flow, the extrapolation, the foreground, the final object partition.

- splitting objects that are not coherent anymore;
- detecting new object that appeared for the first time in the current frame;
- assigning IDs to pixels which are in the foreground according to the foreground-background separation but have no IDs reasoned from the extrapolation phase.

The algorithms we devise to complete these steps are described in details in the next section.

4 ALGORITHMS

4.1 Optical Flow

The optical flow pass we use is a block matching algorithm organized in a coarse-to-fine way similar to the well known Bouguet's (Bouguet, 2000) implementation of the Lucas–Kanade window registration scheme (Lucas and Kanade, 1981). This method had been often discarded in application to dense optical flow due to complications that arise when tracking objects with low texture or frequent occlusions. By carefully choosing appropriate features to track one can limit the negative influence of the aperture problem, but this in general results in sparse optical flow estimation (Tomasi and Kanade, 1991)(Shi and Tomasi, 1993). Other methods incorporate many ways to introduce a global constraint of smoothness (Horn and Schunck, 1981). This solves the aperture problem but on the other hand tends to distort information where flow discontinuities appear. It is also computationally more expensive as global constraints arise and the solution cannot be tackled locally. State of the art optical flow algorithms (Bruhn et al., 2005)(Xu et al., 2010) exploit both these ideas with great accuracy, but are prohibitively slow and do note seem to fit for GPGPU architectures. In order to compute dense optical flow with attention to fine object silhouette tracking we introduced improvements to the pyramidal scheme of (Bouguet, 2000).

4.1.1 Basic Definitions

The optical flow algorithm processes the two consecutive images from the video stream L, C and an identifier map ID that contains the object partition of L. The output consists of a matrix of size $width \times height$ containing pairs: $(u,v) \in \mathbb{Z}^2$ of displacements computed for each pixel that belongs to an object.
In the first step two pyramids of image miniatures are created for L and C. Let us denote these image miniatures by L_i and C_i $(0 \leq i \leq l)$. Each of the $l+1$ levels is a matrix containing extended pixel touples, each level half the width and half the height of the previous. We will refer to the level 0 as the top and to the level l as the bottom. The extended pixel touples contain three values representing the color components r, g, b and two additional values h and v for the horizontal and vertical gradient values. In order to downsize the images we use a small Gaussian kernel. An auxiliary pyramid of identifiers, denoted ID_i, is created from the ID map. The selection of the pixel's identifier is performed by choosing the most frequent identifier from the four pixels directly above in the higher pyramid level.
For the window registration algorithms we will use a normalized dissimilarity measure, based on a componentwise L_1 norm, that compares pixels' r-neighborhoods (for a given radius r).

$$d_{IJ}(p_1,p_2) = \sum_{v \in \{-r,\ldots,r\}^2} \frac{\|I[p_1+v]-J[p_2+v]\|}{(2r+1)^2} \quad (1)$$

4.1.2 Self-dissimilarity

The aperture problem arises most commonly from the appearance of two types of regions in the analyzed

images: large spots with low or none texture (e.g. solid blocks of one color) and regions with repeating self-similar patterns (e.g. a checkered fabric of ones clothing). The dissimilarity between windows on consecutive frames is low and near constant in the local neighborhood or has multiple regular minimums in those parts of the image. This leads to random optical flow estimation when we minimize the dissimilarity in order to find the proper window registration. To prevent such behavior we must first detect which regions hold those unwanted properties. For a given radius r we define a pixel's self-dissimilarity as:

$$sd_I(p) = \sum_{v \in \{-r,\ldots,r\}^2} d_{II}(p, p+v) \quad (2)$$

This quantity tells us weather a pixel's local neighborhood is similar to many such neighborhoods in near proximity. High self-dissimilarity implies the pixels neighborhood is unique, low self-similarity hints us that the pixels neighborhood might be mistaken by a similar neighborhood nearby. Our experiments have shown that in the areas of low self-dissimilarity the standard unmodified optical flow algorithm often finds illusionary movement where none has actually happened, or detects no movement where there has been some. The choice of using average dissimilarity rather than minimum was based on experiments conducted. The minimum of dissimilarities was much more influenced by image noise and resulted in less informative level sets.

For a given limit of dissimilarity lim we compute a pyramid of matrices SD_i matching the sizes of the image and ID pyramids, that contains self-dissimilarity information from the pyramid L_i. We start at the bottom and proceed to the top. The resulting level-0 self-dissimilarity map SD_0 describes the regions of the image in terms of susceptibility to the aperture problem. A level-0 pixel (i.e. $SD_0[x,y] = 0$) has local neighborhoods in every image in the image pyramid at least lim dissimilar. Similarly: a level k pixel (i.e. $SD_0[x,y] = k$) has dissimilarity at least lim in the pyramid levels l up to k.

4.1.3 Window Scaling and Object Masking

Our algorithm will utilize a registration windows of different sizes. We incorporate the scaling factor c into the dissimilarity measure d_{IJ}:

$$d_{IJ}(c, p_1, p_2) = \sum_{v \in \{-r,\ldots,r\}^2} \|I[p_1 + cv] - J[p_2 + cv]\| \quad (3)$$

Moreover, in order to improve the accuracy of the window registration in regions with motion occlusion we decided to incorporate an additional constraint to the dissimilarity measuring function. Optical flow methods like (Sun et al., 2010) try to segment the image based on coherency of optical flow, we use the object assignment in a similar manner. For a given pixel, we take into account only those pixels from it's neighborhood that belong to the same object. If a pixel has an ID set (and only those are processed when computing the optical flow) we consider only those pixels from the r-neighborhood that share the same ID.

Figure 3: The self-dissimilarity map: pixel values ranging from 0 (blue) to 5 (red).

4.1.4 Coarse to Fine Window Registration

In the main part of our optical flow algorithm we find the displacements with a dynamic window registration approach. Similar concept of adaptive window sizes and shapes has been mentioned in (Kanade and Okutomi, 1994)(Yang et al., 2004). In the following we will use a new variable s which is to be fixed afterwards due to some experiments. At each level we limit ourselves to integer displacements candidates $v \in \{-1,0,1\}^2$. With $l+1$ pyramid levels this results in maximal displacements of 2^l in total. At the bottom, for every pixel we choose s best displacements that minimize the dissimilarity between the local neighborhoods in the consecutive frames. At levels $l-1$ through 0 we utilize the s best candidates from the level directly below as starting offsets for the displacement vectors. We use the self-dissimilarity map to scale the window when required. If processing a pixel that has the self-dissimilarity level higher than the currently processed pyramid level we need to make the window larger.

For performance reasons we calculate the optical flow only for the pixels where an object has been discovered. Our experiments show that for the sake of accuracy it is useful to rise the number of samples that are compared when computing dissimilarity with a bigger window. In most of our tests 6 levels of the

image pyramid were sufficient to detect the largest displacements. Considering that a pixel at the bottom level would represent a 32×32 pixel square at the highest resolution, we increase the number of samples in the d_{IJ} dissimilarity measure by a factor of 4 up to 16.

The nature of the other components in the tracker allows us to limit the search to integer displacements. Most differential optical flow algorithms find displacements with sub-pixel precision. This often requires bilinear interpolation as pixel values need to be resolved at real coordinates. Our experiments have shown that $s = 3$ not only compensates this lack of precision in the lower levels, but in fact often gives better results.

Figure 4: Behavior of optical flow algorithms on regions with low texture: left – pyramidal LK, right – our method.

4.2 Extrapolation

The main task of this algorithm is to predict where objects detected in the previous frame are going to appear in the current one. We do this in a rather straightforward manner. To extrapolate a location of an object we process all pixels belonging to it and translate them by vectors computed during the optical flow phase. Apart from the object partition, from the previous frame we get the confidence value in each pixel. During the extrapolation phase we will extrapolate them as well, while the section 4.4 will elaborate in detail on how these confidence values are initiated in the first place. After some experiments we have developed two heuristics which improve the quality of the extrapolation.

The optical flow computed using our method falls victim to some irregularities and in each frame a fraction of pixels is extrapolated in the wrong direction. To prevent this, we check for each pixel whether it's optical flow vector is close enough to the average optical flow calculated in the pixel's neighborhood. If this condition fails we do not extrapolate the given pixel at all.

Two pixels from the previous frame (possibly belonging to two different objects) can be extrapolated to the same pixel in the current frame. It means that one object occludes another and we need to decide which of them is closer to the camera. In order to resolve this we assume, without losing of generality, that the camera is in an upright orientation. Thus we assume that an object located lower in the image is also closer. This method performs fine when object movement is limited to a plane, or close to a plane. Many surveillance scenarios allow such an assumption. More complicated tracking cases, where the objects can move freely in all three dimensions, would require a different method.

4.3 Statistical Background/Foreground Detection

In order to reinforce the information coming from the extrapolation phase we detect foreground objects by analyzing statistical properties of the video stream. The foreground detection module maintains a long term model of the background that contains the color value mean and standard deviation for each pixel. Apart from the long term model we keep two short term statistics (mean and standard deviation) that are gathered over the span of a limited number of frames (say, by 0.5 sec). The long term color statistics are used to decide weather a pixel from a new frame belongs to the foreground. The short term parameters inform us about the volatility of the pixel, which is used to determine the background learning speed. Additionally, we forbid changes to the background model in the regions where the extrapolation phase has already predicted an object.

The short term parameters are updated componentwise, by means of a moving average, with a constant rate every time a new frame appears. The rate is high (i.e. 0.1) in order to accumulate information over a short period. The long term parameters are updated componentwise with a much lower learning rate (i.e. 0.01) that also depends on the volatility of the pixel and the contents of ID'. If volatility is high or we see that the region belongs to an object, the learning rate drops significantly. If the short term parameters are stable, we increase the long term learning rate.

In order to detect regions belonging to the foreground the difference between the color values in the frame and the background model is measured and thresholded. The long term deviation is used to determine the threshold levels. We also introduce a constant additive and a constant multiplicative factors that can be used to scale the deviation, and control the background-foreground separation sensitivity.

4.4 Final Corrections

The purpose of this phase is to combine data we acq-

uired from the extrapolation phase and the background-foreground separation and then utilize it to introduce corrections in the predicted ID' map of the current frame.

The algorithm consists of three steps, which are preceded by computing new foreground map. A pixel is said to be in the foreground if it belongs to any extrapolated object or the statistical foreground.

4.4.1 Splitting Objects

This step is performed to assure that every extrapolated object is coherent.

First, we find the connected components of the foreground map. Each foreground pixel is connected to its four neighbors and the resulting graph is a subgraph of a 2D-grid.

Then, for each extrapolated object we decide which component it belongs to and remove parts of this object from the remaining. We rank candidate components summing confidence values of pixels belonging to the intersection of this component and a given object.

The parts of the object that lie outside of the highest ranked connected component are subtracted from the object.

4.4.2 Detecting New Objects

In this step we detect objects that were not present on the previous frame. These are objects that appeared in the view at this moment or were tracked as a part of another object and were detached from it in the previous step. If there exists a connected component that has an empty intersection with all the extrapolated objects we assign a new unique identifier to all the pixels inside and set their confidence value to 1.

4.4.3 Filling Gaps

We define a gap as a pixel which is believed to belong to the foreground but has no identifier assigned. Usually, at this stage of processing there are still such pixels left. We assign them to an object with a procedure that searches the ID' map in a breadth-first manner. For every gap pixel (x,y) we check its eight neighbors and find the most frequent ID among them. If this ID appears at least three times, we assign it to this gap pixel. Pixel's new confidence is set to the difference between the average confidence of neighbors with the chosen ID and the second best. If such difference turns out to be negative, we leave the gap pixel unchanged.

This procedure is iterated until no gap pixel changes its identification.

5 IMPLEMENTATION DETAILS

The methods described have been prototyped in C++ and tested on x86 CPUs. The algorithms have been then ported to NVIDIA CUDA environment. We have implemented the foreground separation, the optical flow, extrapolation and code related to processing the foreground connected components on the GPU. The only part that relies on CPU computation is the gap fixing phase that requires a breadth-first approach. Although there are BFS algorithms on GPGPUs we have not decided to implement them for simplicity reasons. The overhead related to synchronizing GPU and CPU execution, transferring partial data and running BFS on the CPU has no major influence on overall performance.

The foreground separation proved to be easily parallelized, as pixels could be processed independently. The optical flow phase is the most time consuming part of the algorithm, thus its efficient implementation was the biggest challenge. The problem was memory bandwidth constrained and required careful attention when reading and writing data. A number of approaches has been developed in order to make coalesced memory accesses possible. The optical flow code had a deeply nested structure that had to be properly unrolled for performance reasons. The performance tuning of the optical flow required a good balance between the shared memory usage and the number of simultaneously working blocks.

6 RESULTS

The figures at the end present the object segmentation produced from various test scenarios. The scenario depicted in the first figure shows a group of 6 persons involved in complicated occlusions. The dimensions of the image are 800×600 running at 15 frames per second. The scenarios from the two middle figures are taken from the PETS 2006 workshop datasets. These streams have PAL resolution (i.e. 720×576) and are recorded at 25 frames per second. The last scenario was recorded with a 960×640 frame size at 12.5 frames per second.

Our software run on a Tesla C2050 GPU reaches sustained real-time performance in these scenarios. The average frame processing time varies from 15 to 25 milliseconds. The performance is greatly dependent on the optical flow phase and thus on the total area of tracked objects.

We have also tested the optical flow alone on frames in PAL resolution counting displacement vectors in every pixel. The processing time of 200 mil-

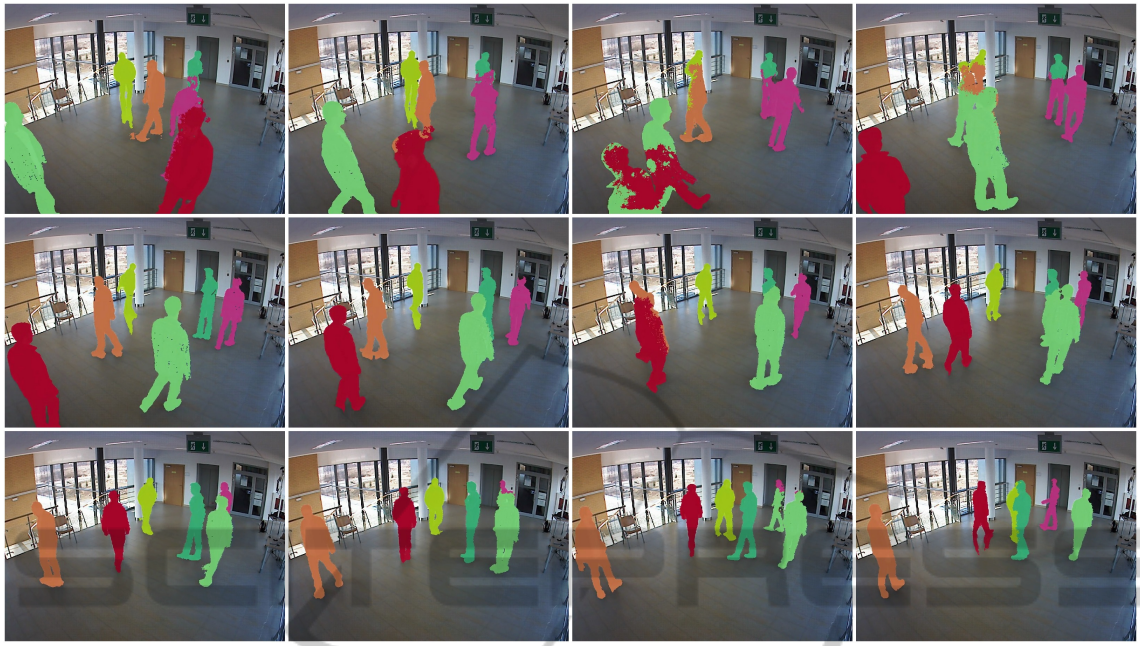

Figure 5: 6-person occlusions.

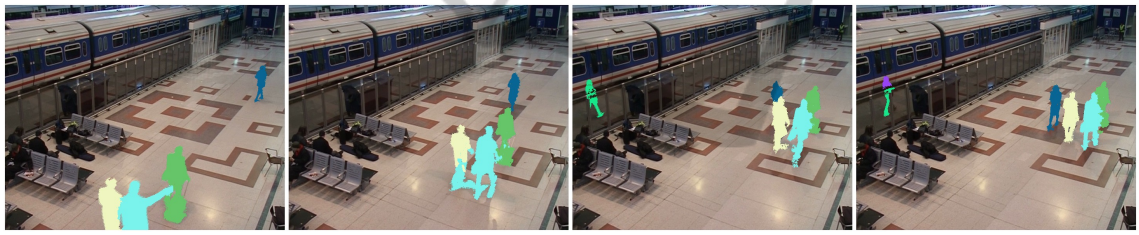

Figure 6: PETS 2006 dataset S1, camera 3.

Figure 7: PETS 2006 dataset S1, camera 4.

Figure 8: Parking lot.

liseconds is the pessimistic case we might be facing.

The prototype of our algorithms has been implemented as a pure CPU solution. In simpler scenarios (i.e. the parking lot) it reached near real-time performance when run on a multicore Intel Xeon X5650 processor.

7 FURTHER WORK

Our tracker is a low-level solution and in order to improve the detection and tracking quality higher level logic might be implemented. In particular such logic could observe the objects in the context of a longer period of time, maintaining its history.

Our future work will focus on following issues:

- When a tracked person hides behind an obstacle and then reappears it is detected as a completely new object.
- Large number of objects appearing simultaneously in the stream results in lower tracking quality and performance, especially in cases with complicated occlusions. There is need for an algorithm for deciding which of the tracked objects can be ignored (e.g. tracking only humans or vehicles).
- Some surveillance scenarios include monitored zones covered by more than one camera. Combining data from multiple trackers can lead to better results.

With the above issues resolved our tracker together with those high level components might be considered as an important part of a robust surveillance system.

ACKNOWLEDGEMENTS

The authors would like to thank the PETS workshops organizers for publishing the datasets we extensively used in our tests.

REFERENCES

Bouguet, J.-Y. (2000). Pyramidal implementation of the lucas kanade feature tracker description of the algorithm.

Bruhn, A., Weickert, J., and Schnörr, C. (2005). Lucas kanade meets horn schunck: Combining local and global optic flow methods. *International Journal of Computer Vision*.

Bugeaue, A. and Pérezz, P. (2008). Track and cut: Simultaneous tracking and segmentation of multiple objects with graph cuts. *Journal on Image and Video Processing*.

Donoser, M., Arth, C., and Bischof, H. (2007). Detecting, tracking and recognizing license plates. In *Proceedings of the 8th Asian conference on Computer vision - Volume Part II*, Berlin, Heidelberg. Springer-Verlag.

Feris, R., Siddiquie, B., Zhai, Y., Petterson, J., Brown, L., and Pankanti, S. (2011). Attribute-based vehicle search in crowded surveillance videos. In *Proceedings of the 1st ACM International Conference on Multimedia Retrieval*, New York, NY, USA. ACM.

Horn, B. and Schunck, B. (1981). Determining optical flow. *Artifical Intelligence*.

Kanade, T. and Okutomi, M. (1994). A stereo matching algorithm with an adaptive window: Theory and experiment. *IEEE Trans. Pattern Anal. Mach. Intell.*

Karlsson, S., Taj, M., and Cavallaro, A. (2008). Detection and tracking of humans and faces. *Journal on Image and Video Processing*.

Lucas, B. and Kanade, T. (1981). An iterative image registration technique with an application to stereo vision. In *Proceedings of the 7th International Joint Conference on Artificial Intelligence - Volume 2*, San Francisco, CA, USA. Morgan Kaufmann Publishers Inc.

Makris, A., Kosmopoulos, D., Perantonis, S., and Theodoridis, S. (2011). A hierarchical feature fusion framework for adaptive visual tracking. *Image Vision Comput.*

Shi, J. and Tomasi, C. (1993). Good features to track. Technical report, Cornell University, Ithaca, NY, USA.

Sun, D., Sudderth, E., and Black, M. J. (2010). Layered image motion with explicit occlusions, temporal consistency, and depth ordering.

Tomasi, C. and Kanade, T. (1991). Shape and motion from image streams: a factorization method - part 3 detection and tracking of point features. Technical report, Pittsburgh, PA, USA.

Wu, B. and Nevatia, R. (2007). Detection and tracking of multiple, partially occluded humans by bayesian combination of edgelet based part detectors. *International Journal of Computer Vision*.

Xu, L., Jia, J., and Matsushita, Y. (2010). Motion detail preserving optical flow estimation. In *Computer Vision and Pattern Recognition*. IEEE Computer Society.

Yang, R., Pollefeys, M., and Li, S. (2004). Improved real-time stereo on commodity graphics hardware. In *Proceedings of the 2004 Conference on Computer Vision and Pattern Recognition Workshop (CVPRW'04) Volume 3 - Volume 03*, Washington, DC, USA. IEEE Computer Society.

Yilmazr, A., Javed, O., and Shah, M. (2006). Object tracking: A survey. *ACM Computing Survey*, 38.

Zweng, A. and Kampel, M. (2009). High performance implementation of license plate recognition in image sequences. In *Proceedings of the 5th International Symposium on Advances in Visual Computing: Part II*, Berlin, Heidelberg. Springer-Verlag.